contribution which these molecules make to the total population of green-emitting species.

In terms of the rigid matrix perturbation of a pseudo-Jahn–Teller potential depicted in Figure 7, this explanation suggests that all molecules in the ensemble are described by the same intramolecular potential (solid line) but that the perturbation (dotted line) varies according to the particular site occupied by a given solute molecule. Solute species experiencing a large rigid matrix perturbation populate green-emitting levels only, while those experiencing a small perturbation may populate red-emitting levels. Thus, modification of the model for the rigidochromic effect based on a pseudo-Jahn–Teller potential by introduction of a variable rigid matrix induced potential is capable of accounting for the decay phenomena encountered in this study.

Acknowledgment is made to the Committee on Research of the University of California, Santa Barbara, for support of this research.

References and Notes

(1) (a) M. K. DeArmond and J. E. Hillis, *J. Chem. Phys.*, **54**, 2247 (1971); (b) *J. Lumin.*, **4**, 273 (1971).
(2) M. K. DeArmond, *Acc. Chem. Res.*, **7**, 309 (1974).
(3) G. A. Crosby, *Acc. Chem. Res.*, **8**, 231 (1975).
(4) C. M. Flynn, Jr., and J. N. Demas, *J. Am. Chem. Soc.*, **96**, 1959 (1974); **97**, 1988 (1975).
(5) R. Ballardini, G. Varani, L. Moggi, and V. Balzani, *J. Am. Chem. Soc.*, **99**, 6881 (1977).
(6) (a) R. J. Watts and G. A. Crosby, *J. Am. Chem. Soc.*, **93**, 3184 (1971); (b) *ibid.*, **94**, 2606 (1972); (c) *Chem. Phys. Lett.*, **13**, 619 (1972).
(7) R. J. Watts, G. A. Crosby, and J. L. Sansregret, *Inorg. Chem.*, **11**, 1474 (1972).
(8) R. J. Watts, J. S. Harrington, and J. Van Houten, *J. Am. Chem. Soc.*, **99**, 2179 (1977).
(9) R. J. Watts, T. P. White, and B. G. Griffith, *J. Am. Chem. Soc.*, **97**, 6914 (1975).
(10) J. A. Broomhead and W. Grumley, *Inorg. Chem.*, **10**, 2002 (1971); *Chem. Commun.*, 1211 (1968).
(11) L. H. Berka and G. E. Philippon, *J. Inorg. Nucl. Chem.*, **32**, 3355 (1970).
(12) M. M. Muir and W. L. Huang, *Inorg. Chem.*, **12**, 1930 (1973).
(13) R. Ballardini, G. Varani, L. Moggi, V. Balzani, K. R. Olson, F. Scandola, and M. Z. Hoffman, *J. Am. Chem. Soc.*, **97**, 728 (1975).
(14) R. Ballardini, G. Varani, L. Moggi, and V. Balzani, *J. Am. Chem. Soc.*, 7123 (1974).
(15) J. N. Demas, E. W. Harris, C. M. Flynn, Jr., and D. Diemanti, *J. Am. Chem. Soc.*, **97**, 3838 (1975).
(16) G. A. Crosby, R. J. Watts, and D. H. W. Carstens, *Science*, **170**, 1195 (1970).
(17) J. N. Demas and G. A. Crosby, *J. Am. Chem. Soc.*, **92**, 7262 (1970); **93**, 2841 (1971).
(18) J. Van Houten and R. J. Watts, *J. Am. Chem. Soc.*, **97**, 3843 (1975).
(19) L. S. Forster in "Concepts of Inorganic Photochemistry", A. W. Adamson and P. D. Fleischauer, Ed., Wiley, New York, N.Y., 1975.
(20) J. D. Petersen, R. J. Watts, and P. C. Ford, *J. Am. Chem. Soc.*, **98**, 3188 (1976).
(21) D. H. Carstens and G. A. Crosby, *J. Mol. Spectrosc.*, **34**, 113 (1970).
(22) R. J. Watts and J. Van Houten, *J. Am. Chem. Soc.*, **96**, 4334 (1974).
(23) M. Wrighton and D. L. Morse, *J. Am. Chem. Soc.*, **96**, 998 (1974).
(24) M. S. Wrighton and P. J. Giordano, Abstracts, 173rd National Meeting of the American Chemical Society, New Orleans, La., March 21–25, 1977, No. INOR-91.
(25) P. J. Giordano, S. M. Fredericks, M. S. Wrighton, and D. L. Morse, *J. Am. Chem. Soc.*, **100**, 2257 (1978).
(26) B. Dellinger and M. Kasha, *Chem. Phys. Lett.*, **36**, 410 (1975); **38**, 9 (1976).
(27) Y. H. Li and E. C. Lim, *Chem. Phys. Lett.*, **9**, 279 (1971).
(28) J. A. Stikeleather, *Chem. Phys. Lett.*, **24**, 253 (1974).
(29) T. Azumi, *Chem. Phys. Lett.*, 17, 211 (1972).
(30) L. G. Vanquickenborne and A. Ceulemans, *J. Am. Chem. Soc.*, **99**, 2208 (1977).
(31) C. A. Taylor, M. A. El-Bayoumi, and M. Kasha, *Proc. Natl. Acad. Sci. U.S.A.*, **63**, 253 (1969).
(32) M. A. El-Bayoumi, P. Avouris, and W. R. Ware, *J. Chem. Phys.*, **62**, 2499 (1975).
(33) R. O. Gillard, *Coord. Chem. Rev.*, **16**, 67 (1975).
(34) W. C. Galley and R. M. Purkey, *Proc. Natl. Acad. Sci. U.S.A.*, **67**, 1116 (1970).
(35) F. Castelli and L. S. Forster, *J. Am. Chem. Soc.*, **95**, 7223 (1973).
(36) C. Conti and L. S. Forster, *J. Am. Chem. Soc.*, **99**, 613 (1977).
(37) W. Halper and M. K. De Armond, *J. Lumin.*, **5**, 225 (1972); *Chem. Phys. Lett.*, **24**, 114 (1974).
(38) G. A. Crosby and W. H. Elfring, Jr., *J. Phys. Chem.*, **80**, 2206 (1976).
(39) R. J. Watts and J. Van Houten, *J. Am. Chem. Soc.*, in press.
(40) R. J. Watts, *J. Am. Chem. Soc.*, **96**, 6186 (1974).
(41) R. J. Watts, M. J. Brown, and J. S. Harrington, *J. Am. Chem. Soc.*, **97**, 6029 (1975).
(42) R. J. Watts, B. G. Griffith, and J. S. Harrington, *J. Am. Chem. Soc.*, **98**, 674 (1976); R. B. King, *Adv. Chem. Ser.*, 201 (1976).

Structures of Two Spiroarsoranes and Their Dynamic Implications

Harold Goldwhite* and Raymond G. Teller

Contribution from the Department of Chemistry, California State University, Los Angeles, California 90032. *Received January 27, 1978*

Abstract: The crystal and molecular structures of two spiroarsoranes have been determined by single-crystal x-ray diffraction analyses. The compound 2,2,3,3,7,7,8,8-octamethyl-5-phenyl-1,4,6,9-tetraoxa-5-arsaspiro[4.4]nonane (I) crystallizes in the monoclinic space group $P2_1/c$ with cell constants $a = 9.150$ (5), $b = 12.699$ (8), $c = 17.386$ (7) Å; $\beta = 103.73$ (5)°; $Z = 4$. The geometry about arsenic lies on the Berry coordinate between rectangular pyramidal and trigonal bipyramidal. The compound 5-hydroxy-1,4,6,9-tetraoxa-5-arsaspiro[4.4]nonane (II) crystallizes in the monoclinic space group $P2_1/c$, with cell constants $a = 9.415$ (4), $b = 6.791$ (2), $c = 12.426$ (5) Å; $\beta = 119.11$ (6)°; $Z = 4$. It too has a geometry about arsenic that lies on the Berry coordinate between rectangular pyramidal and trigonal bipyramidal. These structures lead to a reassessment of dynamic nuclear magnetic resonance spectra of these and allied compounds and also show the close parallels between the structures of related arsenic and phosphorus systems.

Introduction

There has been a continuing evolution of our understanding of the geometries and dynamics of five-coordinate compounds of main-group elements. Phosphorus chemistry provides the principal domain of this evolution. Early ideas of an invariable trigonal bipyramidal arrangement gave way to a recognition that distortions toward rectangular pyramidal might occur in some systems. It now appears that there is a whole range of possible structures for five-coordinate phosphorus compounds corresponding to points along the Berry coordinates for intramolecular exchange.[1]

The present work was undertaken to explore whether a similar structural range might exist for five-coordinate arsenic

0002-7863/78/1500-5357$01.00/0

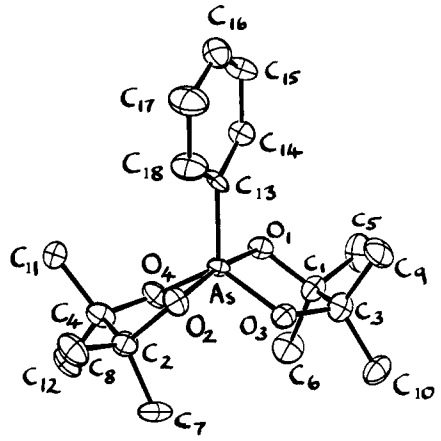

Figure 1. Structure of $C_6H_5As(O_2C_2(CH_3)_4)_2$, compound I. (Hydrogen atoms omitted; 50% probability ellipsoids).

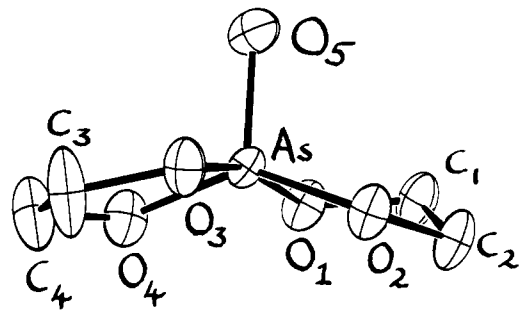

Figure 2. Structure of $HOAs(O_2C_2H_4)_2$, compound II. (Hydrogen atoms omitted; 50% probability ellipsoids).

compounds. Although previous structural studies on arsoranes had revealed uniformly trigonal bipyramidal structures,[2] some dynamic nuclear magnetic spectral studies of arsoranes had led to some conflicts in interpretation between our group and others.[3,4] It seemed to us that better models for the stereochemical analysis of arsoranes were needed and consequently the x-ray crystallographic studies reported here were undertaken.[5]

Experimental Section

Preparation of Compounds. The compound 2,2,3,3,7,7,8,8-octamethyl-5-phenyl-1,4,6,9-tetraoxa-5-arsaspiro[4.4]nonane (I) was prepared by a published method[6] and was crystallized from hexane (mp 108 °C, lit.[6] mp 103 °C). The compound 5-hydroxy-1,4,6,9-tetraoxa-5-arsaspiro[4.4]nonane (II) was also prepared by a published method[7] and was crystallized from ethanol (mp 118 °C, lit.[7] mp 120 °C).

Crystallography. An approximately cylindrically shaped crystal (h = 0.3 mm, r = 0.15 mm) for $C_6H_5As(O_4C_4Me_8)$ (I) and a crystal of approximate dimensions 0.3 × 0.2 × 0.2 mm with ill-defined faces for $HOAs(O_4C_4H_8)$ (II) were selected for data collection after examination of numerous crystals of I and II. Because the crystals of both I and II are hygroscopic they were mounted in thin-walled capillaries. Preliminary crystallographic experiments and data collection were carried out on a Syntex $P2_1$ four-circle diffractometer with graphite monochromatized Mo Kα radiation. Least-squares refinement of the diffraction geometry of 15 intense, high-angle ($25° \leq 2\theta \leq 45°$), general reflections resulted in cell constants and an orientation matrix used for data collection. Systematic extinctions $0k0$, $k = 2n + l$, and $h0l$, $l = 2n + l$, uniquely determined the space groups of both compounds as $P2_1/c$. Cell constants and details of data collection and refinement are reported in Table I.

Data were collected in the $\theta/2\theta$ variable scan mode to a 2θ limit of 55.0°, the maximum and minimum scan rates being 29.3°/min and 4.0°/min. (Only a few extremely intense reflections were collected at the maximum scan rate). The scan range for both I and II was 1.0° below Kα_1 to 1.0° above Kα_2, with the background radiation counted at each end of the scan for 0.25 times the total scan time for each reflection. Three standard reflections were measured every 50 measurements. Examination of these revealed a slight decay for II and only minor fluctuations for I. One octant ($+h, +k, +l$) of data was collected for each compound.

Intensities (4305 for I, 1981 for II) were corrected for Lorentz and polarization, and (for II) decay, effects. Scattering factors for As, O, and C were taken from the International Tables for X-Ray Crystallography. Structure factors fulfilling the criteria $F_o > 3\sigma(F)$[8] were retained for subsequent structure analysis and refinement (2432 for I and 1503 for II). The cylindrical nature of the crystals made an absorption correction unnecessary. This was confirmed by performing ψ scans of several reflections near $\chi = 90°$, which showed negligible variation.

A Patterson synthesis revealed the As atomic positions for both structures and successive cycles of structure factor calculations and difference-Fourier synthesis revealed the positions of all nonhydrogen atoms. Three cycles of full-matrix least-squares refinement on all positional and thermal parameters (allowing the As atoms to vibrate anisotropically) and on the scale factor were carried out, followed by eight cycles of block-diagonalized least-squares calculations varying the scale factor and all positional and anisotropic thermal parameters. The function minimized was $\Sigma(\omega(F_o - |F_c|)^2)$. In the final cycle all shifts were less than 0.20 of the estimated standard deviation of the parameter in question. The final agreement factors are R_w = 0.105 for I and 0.077 for II. A final difference-Fourier synthesis revealed only peaks assignable to hydrogen atom positions. As these atoms were not well behaved in subsequent least-squares calculations, they are not included here. The high agreement factors can be traced to the hygroscopic nature of the crystals which resulted in poor crystal quality.

Table I. Crystal Data for I and II

	$C_6H_5As(O_4C_4Me_8)$ (I)	$HOAs(O_4C_4H_8)$ (II)
cell constants		
a	9.150 (5) Å	9.415 (4) Å
b	12.699 (8) Å	6.791 (2) Å
c	17.386 (7) Å	12.426 (5) Å
β	103.73 (5)°	119.11 (6)°
space group	$P2_1/c$ $Z = 4$	$P2_1/c$ $Z = 4$
density calcd	1.18 g cm^{-3}	2.02 g cm^{-3}
obsd	1.20 g cm^{-3}	1.98 g cm^{-3}
data		
collected	4305	1987
used in analysis[c]	2432	1503
agreement factors		
R^a	0.137	0.082
$R_w{}^b$	0.105	0.077

[a] $R = [\Sigma||F_o| - |F_c||/F_o^2]^{1/2}$. [b] $R_w = [\Sigma w||F_o| - |F_c||/\Sigma wF_o^2]^{1/2}$. [c] Atomic scattering factors used in analysis were taken from ref 15.

Computer Programs. Data reduction and structure refinement were carried out on CDC 3150 and 3300 computers at California State University, Los Angeles, with programs written by R.G.T. The programs were as follows: REDUCE was used to transform raw intensities to structure factors; LEAST performed block-diagonalized least-squares calculations; and STAN calculated standard deviations in bond distances and angles. Structure solution was carried out at the University of Southern California computing center using CRYM, an amalgamated crystallographic computing system, written by Dr. R. Marsh and co-workers at the California Institute of Technology.

Nuclear Magnetic Resonance Spectroscopy. ^{13}C spectra were determined on a Bruker WP-90 instrument. For compound I peaks were assigned as follows (10% solution in carbon disulfide; all peak positions given in parts per million downfield from internal $(CH_3)_4Si$): CH_3CO, 24.40 and 24.99 (two singlets); CH_3CO, 76.58 (one peak); C_6H_5, 127.5–132.6. Peak multiplicities were invariant from 309 to 193 K. For compound II (15% solution in $CDCl_3$ or methanol, ^1H spectra confirmed that there was no chemical change of the spiroarsorane in methanol under these conditions): CH_2O, 60.13 (one peak). The peak remained a singlet from 305 to 210 K.

Table II. Fractional Coordinates and Anisotropic Thermal Parameters for I[a]

atom	x	y	z	β_{11}	β_{22}	β_{33}	β_{12}	β_{13}	β_{23}
As	2584 (2)	996 (1)	2248 (1)	56 (2)	32 (1)	24 (1)	−1 (2)	3 (1)	−3 (1)
O(1)	2625 (9)	−325 (6)	2615 (5)	86 (15)	51 (6)	37 (4)	7 (8)	15 (6)	7 (4)
O(2)	3090 (9)	476 (7)	1407 (5)	86 (15)	60 (7)	27 (4)	8 (8)	7 (6)	−3 (4)
O(3)	745 (9)	1009 (7)	2356 (5)	73 (14)	53 (7)	47 (4)	−4 (9)	14 (6)	2 (5)
O(4)	2288 (9)	2248 (6)	1728 (5)	102 (15)	32 (6)	33 (4)	7 (8)	9 (6)	0 (4)
C(1)	1203 (14)	−748 (10)	2624 (7)	76 (22)	74 (12)	30 (6)	9 (13)	5 (9)	3 (6)
C(2)	3359 (16)	1225 (10)	839 (8)	114 (25)	61 (12)	34 (6)	21 (14)	18 (10)	2 (7)
C(3)	253 (15)	233 (10)	2782 (8)	92 (24)	49 (11)	46 (7)	2 (13)	11 (11)	4 (7)
C(4)	2240 (16)	2164 (11)	887 (8)	134 (27)	67 (12)	28 (6)	5 (15)	18 (10)	3 (7)
C(5)	1365 (17)	−1642 (11)	3233 (9)	166 (31)	53 (11)	57 (8)	18 (15)	23 (13)	−16 (8)
C(6)	519 (16)	−1213 (11)	1787 (8)	147 (28)	65 (13)	40 (7)	28 (15)	−1 (11)	20 (7)
C(7)	3025 (16)	678 (11)	27 (8)	124 (26)	92 (14)	31 (6)	−27 (15)	15 (10)	10 (7)
C(8)	5007 (17)	1565 (13)	1097 (9)	83 (26)	116 (16)	51 (8)	−23 (16)	8 (12)	0 (9)
C(9)	−1492 (15)	112 (12)	2493 (9)	66 (24)	78 (13)	53 (8)	−18 (14)	13 (11)	7 (8)
C(10)	670 (17)	535 (12)	3701 (8)	176 (10)	95 (14)	35 (7)	−38 (17)	40 (12)	−13 (8)
C(11)	570 (17)	1864 (14)	445 (9)	93 (27)	126 (17)	43 (8)	24 (17)	−6 (11)	2 (9)
C(12)	2747 (20)	3218 (13)	603 (10)	253 (39)	87 (15)	57 (9)	15 (9)	46 (15)	3 (9)
C(13)	4166 (14)	1509 (9)	3087 (7)	58 (21)	43 (9)	33 (6)	−23 (11)	8 (9)	4 (6)
C(14)	4912 (16)	805 (12)	3679 (8)	125 (26)	76 (14)	41 (7)	6 (15)	−21 (10)	6 (8)
C(15)	6102 (18)	1158 (13)	4301 (9)	159 (31)	102 (16)	53 (8)	−17 (18)	−19 (12)	3 (9)
C(16)	6527 (16)	2231 (12)	4307 (9)	124 (28)	89 (14)	49 (8)	−12 (17)	28 (12)	−7 (9)
C(17)	5747 (16)	2935 (11)	3745 (9)	112 (27)	61 (12)	49 (8)	−22 (15)	0 (11)	−7 (8)
C(18)	4563 (15)	2568 (11)	3121 (8)	120 (27)	67 (12)	37 (7)	−17 (14)	17 (11)	−6 (7)

[a] Anisotropic thermal parameters are of the form $\exp\{-[\beta_{11}h^2 + \beta_{22}k^2 + \beta_{33}l^2 + 2\beta_{12}hk + 2\beta_{13}hl + 2\beta_{23}kl]\}$ for Tables II and III. Standard deviations are given in parentheses in this and subsequent tables. All quantities have been multiplied by 10^4.

Table III. Fractional Coordinates and Anisotropic Thermal Parameters for II

	X	Y	Z	β_{11}	β_{22}	β_{33}	β_{12}	β_{13}	β_{23}
As	2254 (1)	5309 (1)	2937 (1)	126 (1)	124 (1)	73 (1)	−2 (1)	65 (1)	−7 (1)
O(1)	1553 (8)	5356 (9)	4044 (5)	220 (11)	205 (13)	88 (5)	−47 (11)	98 (7)	−25 (7)
O(2)	3778 (7)	7003 (10)	3850 (6)	179 (11)	232 (16)	129 (7)	52 (10)	102 (7)	32 (8)
O(3)	3393 (8)	4871 (9)	2165 (6)	177 (10)	206 (15)	117 (6)	−7 (9)	112 (7)	−5 (7)
O(4)	1827 (7)	2724 (9)	2843 (5)	212 (11)	173 (14)	99 (6)	−14 (9)	103 (7)	−6 (7)
O(5)	0666 (7)	6482 (10)	1745 (5)	205 (11)	274 (18)	79 (5)	−73 (11)	82 (7)	−25 (8)
C(1)	2330 (16)	6840 (18)	4965 (10)	427 (31)	344 (33)	149 (12)	230 (27)	192 (17)	140 (17)
C(2)	3533 (14)	7887 (19)	4797 (10)	257 (22)	382 (37)	152 (13)	131 (23)	127 (14)	131 (18)
C(3)	2369 (12)	1671 (14)	2087 (9)	256 (19)	158 (19)	139 (11)	−8 (15)	142 (12)	−26 (11)
C(4)	2806 (12)	3155 (14)	1398 (8)	255 (20)	210 (23)	118 (10)	13 (17)	129 (12)	−26 (12)
H(1)[a]	0000	7250	1950						

[a] Not refined.

Infrared spectra were determined on a Beckman Acculab 2 spectrometer, calibrated by polystyrene film.

Results and Discussion

Molecular Structure. The atomic parameters for I and II are given in Tables II and III, respectively; perspective views of the molecular forms of I and II in the crystalline state are shown in Figures 1 and 2. Bond angles are given in Tables IV and V and bond lengths, which are unexceptional, in Table VII. When this investigation was initiated, the paradigmatic view of the structure of five-coordinate compounds containing arsenic as a central atom was that they were close to trigonal bipyramidal in form.[2] However, our own spectral observations on some spiroarsoranes,[3] and those of others,[4,9] led us to conclude that a wider range of structural data would be worth gathering on arsoranes.[10] Furthermore, there was accumulating in the literature a variety of structural studies on phosphoranes[1] which indicated that a range of five-coordinate structures might be observed for arsoranes too. The present studies have confirmed that expectation.

In an exemplary series of structural investigations and interpretations of phosphoranes, Holmes and his collaborators have quantified structural deviations from idealized trigonal bipyramidal (TP) and square or rectangular pyramidal (SP, RP) end forms, and have shown, by a number of tests, that most phosphorane structures lie on the Berry pathway for ligand displacement between the idealized end forms.[1] We have followed this approach to analyze the structures we have observed for these two arsoranes. Table IV presents the results of an angle deviation analysis (sum of angles method) for I and Table V a similar analysis for II. This method uses the differences between the angles observed in the central coordination unit and those expected for various ideal structures to test for the extent of deviation from an ideal form. The results for I indicate that this phenylspiroarsorane has a structure closer to TP than to RP but that it is significantly distorted along the Berry pathway from TP toward RP. The results for II show that the hydroxospiroarsorane is closer to RP than to TP and that again the distortions follow the Berry coordinate closely.

Perhaps a better quantitative test of the extent of distortion from an ideal model is that given by the dihedral angle method,[1,11] which compares observed dihedral angles between adjacent triangular faces with those calculated for idealized structures. In Table VI the results of such an analysis are presented. It is in conformity with the angle deviation analysis. Compound I is much closer to TP than to RP while II is somewhat closer to RP than to TP. Both compounds lie along the Berry coordinate; in quantitative terms I is some 16% dis-

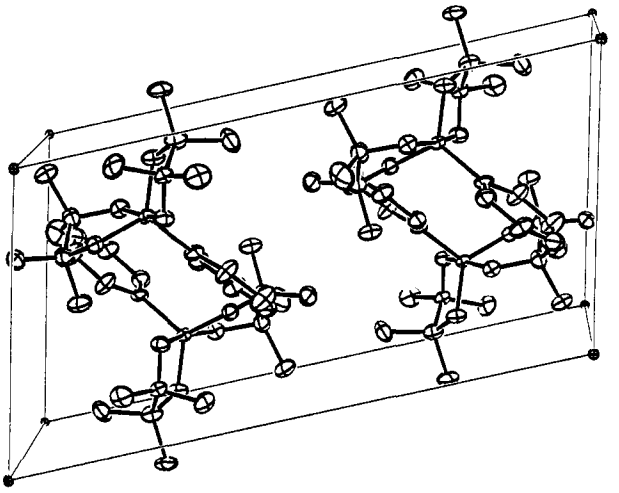

Figure 3. Unit cell of compound I.

Table IV. Angle Deviation Analysis for I

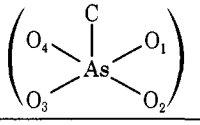

angle[a]	obsd[a]	ΔTP[b]	ΔRP[c]	ΔTR(15)[d]	ΔTR(30)[e]
12	87.4	2.6	2.6	2.6	2.6
34	88.3	1.7	1.7	1.7	1.7
14	87.3	2.7	5.0	2.7	2.6
23	87.5	2.5	4.2	6.1	2.8
1C	117.4	2.6	12.4	12.4	3.3
2C	94.5	4.5	10.5	4.5	4.5
3C	118.0	2.0	13.0	5.9	3.9
4C	95.7	5.7	9.3	5.7	5.7
13	124.6	4.6	25.4	20.1	30.7
24	169.8	10.2	19.8	4.8	14.5
	ΣΔ	39.1[f]	103.9[g]	66.5	72.3

[a] 12 means the angle O_1AsO_2, etc. All angles in degrees; standard deviation for observed angles, 0.3°. [b] Difference between observed angle and corresponding angle in ideal TP; see ref 1, Figure 3, and Table I for further details. [c] Difference between observed and corresponding angles in ideal RP; see ref 1. [d,e] Differences between observed and corresponding angles in 15 or 30° turnstile rotation; see ref 1. [f] Minimum sum of deviations is for TP. [g] 135.4 − g = 31.5°, close to the value f; indicates closeness to Berry coordinates; see ref 1.

torted from TP toward RP and II is 60% distorted from TP toward RP.

Crystal Structure. The unit cell of I is illustrated in Figure 3. There are no particularly unusual features in the crystal packing. Intermolecular contacts are normal. The unit cell of II is shown in Figure 4 and it is clear that the molecules of the hydroxospiroarsorane pack as dimeric units. Although the hydrogen atom of the hydroxo group was not refined in this study, the packing indicates that there is hydrogen bonding in the crystal between the hydroxo hydrogen and a ring oxygen of a neighboring molecule. The intermolecular oxygen-oxygen distances in the dimeric units are 2.77 Å and the geometric environment in the AsOH- - -O fragment is as shown in Figure 5. The OH bond length is 0.97 Å which is exactly as expected for a normal OH bond.[12] The H- - -O hydrogen bond length is 1.86 Å, much less than the sum of the van der Waals radii of hydrogen and oxygen (2.6 Å), strongly suggesting that hydrogen bonding is present.[12] This is supported by infrared spectral studies. A Nujol mull of the crystalline solid shows an

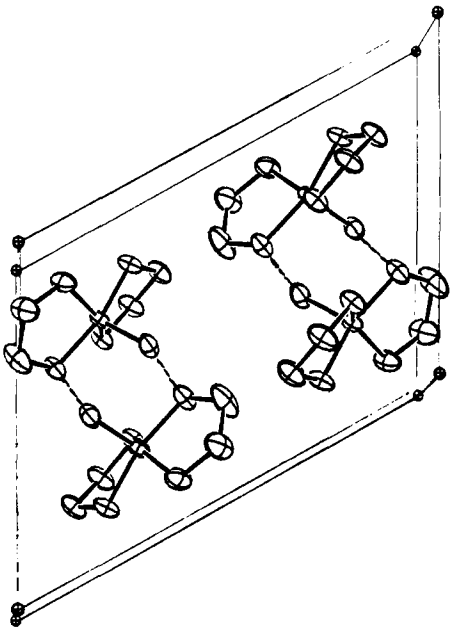

Figure 4. Unit cell of compound II. Dashed lines indicate hydrogen bonding in the dimers.

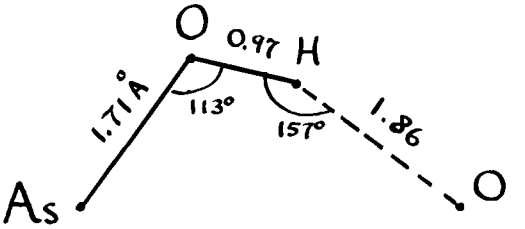

Figure 5. Hydrogen bonding in compound II.

Table V. Angle Deviation Analysis for II

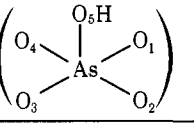

angle[a]	obsd[a]	ΔTP	ΔRP	ΔTR(15)	ΔTR(30)
12	88.4	1.6	1.6	1.6	1.6
34	89.3	0.7	0.7	0.7	0.7
14	85.1	4.9	2.8	4.9	0.4
23	86.6	3.4	4.3	5.2	1.9
15	109.1	10.9	4.1	19.1	19.1
25	96.3	6.3	8.7	6.3	6.3
35	110.5	9.5	5.5	13.4	13.6
45	99.4	9.4	5.6	5.6	14.7
13	140.4	20.4	9.6	4.3	14.9
24	164.0	16.0	14.0	1.0	8.7
	ΣΔ	83.1[c]	56.9[b]	62.1	81.9

[a] Abbreviations as for Table IV. All measurements in degrees, standard deviations for angles, 0.3°. [b] Minimum deviation sum for RP. [c] 135.4 − b = 78.5, close to c, indicating distortion along the Berry coordinate. See ref 1.

intense broad absorption centered at 3180 cm^{-1}, a frequency similar to those observed in organophosphorus compounds containing hydrogen-bonded P-OH- - -O groups.[13] However, a dilute (0.1%) solution of the compound in $CDCl_3$ shows no indication of this band; a new band is seen at 3540 cm^{-1} which

Table VI. Dihedral Angle Analysis for I and II

dihedral angle[a]	obsd (I)	$\Delta(I)_{TP}$[b]	$\Delta(I)_{RP}$[c]	obsd (II)	$\Delta(II)_{TP}$[b]	$\Delta(II)_{RP}$[c]
e_1	59.4	6.3	16.3	65.9	12.8	9.8
e_2	58.3	5.2	17.4	65.9	12.8	9.8
e_3	41.1	12.0	41.1	22.6	30.5	22.6
a_1	102.1	0.6	17.7	111.0	9.5	8.8
a_2	97.6	3.9	21.9	86.2	15.3	10.5
a_3	103.9	2.4	15.9	111.8	10.3	8.0
a_4	103.6	2.1	16.2	113.2	11.7	6.6
a_5	100.3	1.2	24.6	85.1	16.4	9.4
a_6	102.9	1.4	16.9	112.2	10.7	7.6
	$\Sigma\Delta$	35.1[d]	188.0[e]		130.0[f]	93.1[g]
% distortion[h]	16			60		

[a] Symbolism follows that of ref 10. All angles in degrees. [b] Difference between observed angles and those for ideal TP. [c] Difference between observed angles and those for ideal RP. [d,e] 217.7 − e = 29.7, close to d; distortion is along Berry coordinate; see ref 1. [f,g] 217.7 − g = 124.6, close to f; distortion is along Berry coordinate. [h] % distortion along Berry coordinate from TP toward RP = $\Sigma\Delta TP/217.7°$. See ref 1.

Table VII. Observed Bond Lengths (Å)

compd I		compd II	
As-O(1)	1.793 (6)	As-O(1)	1.792 (6)
As-O(2)	1.763 (6)	As-O(2)	1.755 (9)
As-O(3)	1.741 (5)	As-O(3)	1.793 (7)
As-O(4)	1.817 (8)	As-O(4)	1.775 (7)
As-C(13)	1.908 (7)	As-O(5)	1.704 (6)
O(1)-C(1)	1.410 (4)	O(1)-C(1)	1.427 (5)
O(3)-C(3)	1.455 (6)	O(2)-C(2)	1.442 (6)
O(2)-C(2)	1.434 (9)	O(3)-C(3)	1.424 (5)
O(4)-C(4)	1.456 (7)	O(4)-C(4)	1.440 (4)
C(1)-C(5)	1.537 (7)	C(1)-C(2)	1.458 (6)
C(1)-C(6)	1.558 (9)	C(3)-C(4)	1.486 (8)
C(3)-C(9)	1.565 (8)		
C(3)-C(10)	1.599 (8)		
C(2)-C(8)	1.528 (8)		
C(2)-C(7)	1.588 (9)		
C(4)-C(11)	1.587 (8)		
C(4)-C(12)	1.536 (9)		
C(1)-C(3)	1.580 (6)		
C(2)-C(4)	1.588 (7)		
C(13)-C(14)	1.411 (6)		
C(14)-C(15)	1.412 (6)		
C(15)-C(16)	1.416 (7)		
C(16)-C(17)	1.392 (8)		
C(17)-C(18)	1.418 (8)		
C(18)-C(13)	1.390 (9)		

we assign to non-hydrogen-bonded OH, by analogy with those in other organometallic hydroxides.[14]

Dynamic Implications. Earlier discussions of the solution behavior of spiroarsoranes, as studied by ^1H dynamic nuclear magnetic resonance spectroscopy,[3,4] were based on an assumed ideal TP structure for the compounds. It is now apparent that this was an oversimplification. The actual structures observed for I and II suggest that distortions along the Berry coordinate are rather facile for spiroarsoranes, in agreement with our earlier interpretation.[3] We now also have carbon-13 dynamic NMR data which reinforce the conclusions previously drawn from ^1H data. Thus for both I and II, over temperatures ranging from 309 to 193 K for I, and 305 to 210 K for II, only one ^{13}C signal is seen for the carbon atoms of the spiro rings. While accidental isochronicity did seem to be a possible way of explaining the simple ^1H spectra of I and II,[4,9] it seems less plausible an explanation for their simple ^{13}C spectra, in view of the much wider chemical shift range usually found in ^{13}C spectra. We conclude that in these particular compounds there is a facile dynamic process averaging ring carbon atom environments in both compounds. Since the solid state structures of I and II lie so close to the Berry coordinate, we suggest that the dynamic process is distortion along that coordinate. For compound I the earlier discussion still suffices, because in the solid state, at least, it is only 16% distorted from TP. For compound II, which is closer to RP than to TP (60% distorted from TP), we can suggest an alternative mode of dynamic distortion in which the molecule flexes between a structure like that shown in the solid state (Figure 2) and its mirror image, with the RP as the transition state or intermediate. If this process were rapid on the NMR time scale it would average the ring carbon ^{13}C environments. In a recent dynamic NMR study of some acyclic arsoranes this same general point was made,[9] namely, that the observed spectra do not allow deduction as to whether TP, RP, or any intermediate structure is the most stable configuration in solution.

It seems very likely to us that as a wider range of arsoranes is studied by dynamic and structural methods a picture comparable to that found in phosphoranes will emerge, namely, structural types which approach the idealized end forms will be found together with a host of intermediate forms.[1] The correlation of particular molecular features with observed molecular structure in this fascinating group of five-coordinate molecules remains a challenge for the future.

Acknowledgments. We thank James Grey for assistance with some of the preparative chemistry; Professors A. Colville and G. Novak of the Department of Geology, for help with the x-ray data collection; and Professor R. Bau, of the University of Southern California, for the loan of computer programs and a generous donation of computer time. This work was supported, in part, by Grant CA-07182, awarded by the National Cancer Institute, DHEW.

Supplementary Material Available: Tabular listings of structure factor amplitudes for I and II (15 pages). Ordering information is given in any current masthead page.

References and Notes

(1) R. R. Holmes and J. A. Deiters, *J. Am. Chem. Soc.*, **99**, 3318 (1977).
(2) J. P. Crow and W. R. Cullen, *MTP Int. Rev. Sci.*, **4**, 355–412 (1972).
(3) H. Goldwhite, *Chem. Commun.*, 651 (1970).
(4) J. P. Casey and K. Mislow, *Chem. Commun.*, 1410 (1970).
(5) For a preliminary report on the structure of I, see H. Goldwhite, J. Grey, and R. Teller, *J. Organomet. Chem.*, **113**, C1 (1976).
(6) E. J. Salmi, K. Merivuori, and E. Laaksonen, *Suom. Kemistil. B*, **19**, 102 (1946).
(7) B. Englund, *J. Prakt. Chem.*, **120**, 179 (1928).
(8) $\sigma(F) = \frac{1}{2}(C(R[I_S + I_B/BS] + [0.02I_n]^2/I_n)^{1/2}$. BS = background time/scan time; I_S = scan intensity; C = Lorentz, polarization, and decay correction constant; R = scan rate.
(9) A. J. Dale and P. Frojen, *Acta Chem. Scand., Ser. B*, **29**, 362, 741 (1975).
(10) The case for the utility of crystallographic data in interpreting processes in solution has been persuasively argued by H-B. Burgi, *Angew. Chem.*,

Int. Ed. Engl., **14**, 460 (1975).
(11) E. L. Muetterties and L. J. Guggenberger, *J. Am. Chem. Soc.*, **96**, 1748 (1974).
(12) W. C. Hamilton in "Structural Chemistry and Molecular Biology", A. Rich and N. Davidson, Ed., W. H. Freeman, San Francisco, Calif., 1968, pp 467–470.
(13) L. C. Thomas, "Interpretation of the Infrared Spectra of Organophosphorus Compounds", Heyden, London, 1974, Chapter 3.
(14) E. Maslowsky, "Vibrational Spectra of Organometallic Compounds", Wiley, New York, N.Y., 1977, pp 109–110.
(15) "International Tables for X-Ray Crystallography", Vol. III, 2nd ed, Kynoch Press, Birmingham, England, 1965.

Coordination Chemistry of Microbial Iron Transport Compounds. 9.[1] Stability Constants for Catechol Models of Enterobactin

Alex Avdeef, Stephen R. Sofen, Thomas L. Bregante, and Kenneth N. Raymond*

Contribution from the Department of Chemistry and Materials and Molecular Research Division, Lawrence Berkeley Laboratory, University of California, Berkeley, California 94720. *Received October 26, 1977*

Abstract: The stability constants of ferric complexes with several substituted catechol (1,2-dihydroxybenzene) ligands in aqueous solutions of low ionic strength have been determined at 27 °C in the pH range 2–11. These simple compounds are used as models of the catechol-containing iron transport compounds (siderophores) found in microorganisms. Enterobactin, the principal siderophore of enteric bacteria, is a tricatechol and, from the formation constants reported here, is estimated to have a formation constant with ferric ion which is greater than 10^{45}. The stepwise formation constants, K_n, of the catechol ligands reported here are defined as $[ML_n]/[ML_{n-1}][L]$, in units of L mol^{-1}, where [L] is the concentration of the deprotonated catechol ligand. The constants were determined from potentiometric and spectroscopic data and were refined on pH values by weighted least squares. Qualitative examination of electron spin resonance spectra of some of the systems indicated some oxidation of the ligand by ferric ions at pH values as high as 4. The ligands studied included catechol (cat) (log K_1 = 20.01, log K_2 = 14.69, log K_3 = 9.01); 4,5-dihydroxy-*m*-benzenedisulfonate (Tiron) (log K_2 = 15.12, log K_3 = 10.10); 4-nitrocatechol (ncat) (log K_1 = 17.08, log K_2 = 13.43, log K_3 = 9.51); 3,4-dihydroxyphenylacetic acid (dhpa) (log K_1 = 20.1, log K_2 = 14.9, log K_3 = 9.0); and 2,3-dihydroxybenzoic acid (dhba) (log $K_1 \approx$ 20.5). The acid dissociation constants, K_as, were determined also. For the catechol protons these follow: cat (pK_{a_1} = 9.22, pK_{a_2} = 13.0); Tiron (pK_{a_1} = 7.70, pK_{a_2} = 12.63); ncat (pK_{a_1} = 6.65, pK_{a_2} = 10.80); dhpa (pK_{a_1} = 9.49, pK_{a_2} = 13.7); and dhba (pK_{a_1} = 10.06, pK_{a_2} = 13.1). In addition, carboxylate substituents of dhpa and dhba have pK_as of 4.17 and 2.70, respectively. In acidic solution there is evidence of coordination by dhpa via the carboxylate group (which presumably does not involve chelation). Similar coordination by dhba does involve chelation (the same as salicylate) and the system is complicated by mixed-mode coordination of both catechol and salicylate type. In solution, exchange is slow between these two types of coordination following changes in pH.

Introduction

The siderophores (previously called siderochromes)[2] are a class of low molecular weight chelating agents which are manufactured by microorganisms, in response to an iron deficiency, and which facilitate uptake of iron into the organisms. The profound insolubility of ferric hydroxide and the low equilibrium concentrations of ferric ion in biological environments are overcome by the enormous stability and ion selectivity of the ferric siderophore complexes. One important siderophore is enterobactin[3] (Figure 1), the iron sequestering agent for enteric bacteria such as *Escherichia coli*. Since iron is an essential nutrient for all pathogenic bacteria and since the availability of iron often limits the rate of bacterial growth, the siderophores have considerable medical importance.[2] Of particular interest are the formation constants of the ferric siderophore complexes, since these constants define the limits for conditions in which iron will be extracted from other biological ferric complexes in the host organism.

The chelating moieties in enterobactin are catechol (1,2-dihydroxybenzene) groups. Catechol-containing molecules are of widespread biological occurrence and importance. A major class are the catecholamines, which function as neurotransmitters[4] and are of pharmacological use in such diverse areas as the treatment of Parkinson's disease,[5] hypertension,[6] and breast cancer.[7] It has been proposed that the antihistamine action of some of these catechols is related to competition with histamine for the receptor sites, which may be metal ions.[8] Ferric ions can inhibit the constrictor response of adrenaline, an effect attributed to the oxidation of the catechol by the metal.[9] Vanadium catechol complexes have been reported to have nitrogen fixation activity.[10]

It has been recognized for some time that ferric ions can form very stable complexes with catechol ligands.[11] For example, adrenaline can extract iron from ferritin.[9] Although there have been several studies of the stabilities of ferric complexes with catechol-containing ligands,[12-20] no general correlation of the stability of these complexes with electronic and steric substituent effects of the ligands has been found. In acidic aqueous solutions (pH 1–2), Mentasti and co-workers[19,20] studied the formation of 1:1 (metal to ligand) ferric complexes with a wide variety of catechols using stopped-flow and spectroscopic techniques.

Our interest in the coordination chemistry of enterobactin has led to the study of simpler catechol complexes as models for the more complicated biological molecules.[21] The extensive hydrolysis of enterobactin in even mildly basic solutions (pH >8), involving the cleavage of the ester linkages, precludes the direct determination of its proton dissociation constants. Moreover, its ferric complex appears to be oxidatively unstable in acidic medium. It was thus important to establish, by the use of readily available simple compounds, (1) a realistic lower bound for the formation constant of ferric enterobactin and related biological compounds, (2) the extent and nature of the

0002-7863/78/1500-5362$01.00/0